Vortex creep and critical current densities J_c in a 2 m thick $SmBa_2Cu_3O_{7d}$ coated conductor with mixed pinning centers grown by co-evaporation

2016 Supercond. Sci. Technol. 29 075011

(http://iopscience.iop.org/0953-2048/29/7/075011)

IOP Publishing Superconductor Science and Technology
Supercond. Sci. Technol. 29 (2016) 075011 (7pp) doi:10.1088/0953-2048/29/7/075011

Vortex creep and critical current densities J_c in a 2 μm thick $SmBa_2Cu_3O_{7-d}$ coated conductor with mixed pinning centers grown by co-evaporation

N Haberkorn[1], Y Coulter[2], A M Condó[1], P Granell[3], F Golmar[3,4], H S Ha[5] and S H Moon[6]

[1] Consejo Nacional de Investigaciones Científicas y Técnicas, Centro Atómico Bariloche, Av. Bustillo 9500, 8400 San Carlos de Bariloche, Argentina
[2] Los Alamos National Laboratory, Los Alamos, NM 87545, USA
[3] INTI-CMNB, CONICET, Av. Gral Paz 5445 (B1650KNA), San Martín, Buenos Aires, Argentina
[4] Escuela de Ciencia y Tecnología, UNSAM, Campus Miguelete, (1650), San Martín, Buenos Aires, Argentina
[5] Korea Electrotechnology Research Institute, Sungjoo-dong, Changwon 641-120, Korea
[6] SuNAM Co. Ltd, Ansung, Gyeonggi-Do 430-817, Korea

E-mail: nhaberk@cab.cnea.gov.ar

Received 12 February 2016, revised 16 May 2016
Accepted for publication 20 May 2016
Published 3 June 2016

Abstract

We report the critical current densities J_c and flux creep rates in a 2 μm thick $SmBa_2Cu_3O_{7-\delta}$ coated conductor produced by co-evaporation. The sample presents strong pinning produced by correlated disorder (CD) (boundaries between growth islands, dislocations and twin boundaries) as well as random nanoparticles. Correlated pinning along the c-axis was evidenced due to the appearance of a large peak in the angular critical current, centered at $\mathbf{H} \| c$. The analysis of the critical current density J_c (with the magnetic field applied parallel ($\mathbf{H} \| c$) and at 45° of the c-axis ($\mathbf{H} \| 45°$)) indicates that CD assists pinning throughout the temperature range. For all temperatures and at both angles the in-field dependence of J_c exhibits a power-law behavior. The contribution of CD drops when the field is rotated to intermediate angles between the c axis and a–b axis (i. e. $\mathbf{H} \| 45°$), which derives in a reduction of the absolute J_c value and poorer in-field dependences. The flux creep rate depends on the angle and its values remain approximately constant within the power-law regime. For $\mathbf{H} \| c$ and $\mathbf{H} \| 45°$ and for magnetic fields lower than 20 kOe, the flux relaxation presents characterizing glassy exponents $\mu = 1.70$ and $\mu = 1.32$, respectively.

Keywords: coated conductors, vortex dynamics, glassy exponents

1. Introduction

The discovery of high-temperature superconductors (HTS) in 1986 and 1987, particularly $RBa_2Cu_3O_{7-d}$ (RBCO; R = Y, Gd, Sm, Gd) with superconducting critical temperature $T_c \approx 92$ K sparked great interest in the use of HTS materials in practical applications, such as transmission lines, motors and generators [1–4]. The potential applications of HTS have been enhanced by the development of coated conductors (CCs). This term refers to superconducting films on flexible substrates with lengths over 1 km. CCs have been successfully grown by chemical and physics methods [5–9]. For some applications of CCs it is necessary to optimize critical current densities J_c at low fields (e.g., for fault current limiters), whereas for others (e.g., motors or magnet inserts) it is necessary to optimize J_c for higher fields. The J_c values in thin films are affected by thickness [2] and microstructure of the samples [10]. In view of the requirements to enhance the

superconducting performance of these epitaxial films, correlating defect structure with vortex pinning efficiency in HTS films and CCs has been one of the major concerns in recent years [10, 11]. The microstructure of CCs is related to the processing parameters and to the method employed in the synthesis [6, 7, 12–14].

Microstructural defects are the primary determining factors for the values of J_c in HTS after electronic anisotropy. Crystalline defects such as fine precipitates of non-superconducting phases [6, 15], dislocations, oxygen vacancies and twins (TBs), among others, act as pinning centers [2, 16]. Their effectiveness at different temperatures, magnetic field and angle depends on their geometry and density [17]. Point defects, usually referred to as weak pinning centers, are particularly effective for temperatures below 40 K [17–19]. Large defects, usually referred to as strong pinning centers, are effective throughout the whole range of temperature [12, 14, 20, 21]. Pinning by strong pinning centers can be isotropic (i.e. nanoparticles NPs) [14, 20, 22] or correlated (extended defects, i.e. columnar defects by secondary phase precipitation or heavy ion irradiation, dislocations and TBs) [12, 15, 23]. Correlated disorder (CD) reduces the rapid suppression of the in-field J_c, particularly when the magnetic field is applied parallel to the defects. Different strategies based on artificially designed pinning landscapes (including weak and strong pinning centers) have been used to improve both, absolute and in-field J_c values [12, 15, 18, 19]. Their effectiveness is finally limited by thermally activated flux-creep [18, 24].

The optimization of J_c through identification and tailoring of defect microstructures which lead to high pinning and reduced vortex creep is a challenge in the design of CCs. Vortex motion in HTS occurs as a result of a rich variety of low energy depinning excitations, which depend on the temperature T, magnetic field H, non-equilibrium current density J and on the type of pinning centers [12]. The giant flux creep rate observed using magnetic relaxation of the persistent currents has been described according to the collective vortex creep model based on the elastic properties of the lattice [25]. According to vortex-glass and collective creep theories, the effective activation energy as a function of current density (J) is given by

$$U(J) = \left(\frac{U_0(T)}{\mu}\right)\left[\left(\frac{J_c}{J}\right)^{\mu} - 1\right], \tag{1}$$

where $U_0\ (T) = U_0 G(T)$ is the scale of the pinning energy (with $G(T)$ a thermal factor, U_0 is the characteristic energy, J_c is the critical current density, and $\mu > 0$ is the characteristic glassy exponent. The μ value is a parameter that characterizes the creep rate is usually is around 1. Its value depends on magnetic field, temperature and current [26]. The time decay of J is given by the interpolation formula

$$J = J_c\left[1 + \frac{\mu T}{U_0}\ln(t/t_0)\right]^{-1/\mu}, \tag{2}$$

where t_0 is a characteristic time. The normalized creep rate $S = -\delta \ln J/\delta \ln t$ that result from the interpolation equation and the nonlinear dependence of $U\ (J)$ is

$$S = \frac{T}{U_0 + \mu T \ln(t/t_0)} = \frac{T}{U_0}\left(\frac{J}{J_c}\right)^{\mu}. \tag{3}$$

For cuprates, the theory explains experimental S values and the origins of the plateau with $S \approx 0.02$ to 0.03 often observed at intermediate temperatures [26]. The plateau appears in the limit $U_0 \ll \mu T \ln t/t_0$ and it corresponds to $S \approx \frac{1}{\mu \ln t/t_0}$. There are no theoretical predictions of the μ values in the case of pinning produced by combinations of strong defects of differing geometry, typically present in films and CCs [2, 11, 27]. Usually, HTS superconductors present a plateau with $S \sim 0.02$ to 0.03 [12, 14, 18, 19, 28, 29]. It was observed that strong pinning centers reduce the flux creep rates at high temperatures [28, 29]. The resulting J_c cannot be inferred as a simple addition of pinning centers reducing the vortex motion [12]. The strength of the pinning potential and the type of depinning excitation (with a specific μ value) depend on the pinning landscape and the J_c/J_0 ratio (being J_0 the depairing critical current density). The actual understanding of the glassy mechanisms for mixed pinning landscapes is very limited. In particular, the methods to constrain the detrimental effects of thermal fluctuations are almost unexplored. Systematic comparisons of the resulting J_c and the glassy exponent μ for specific pinning landscapes have not been performed. Investigating vortex dynamics in CCs developed by different methods (with different pinning landscapes) is relevant for a better understanding of pinning mechanisms, which may lead to the discovery of more general strategies to reduce creep [30].

In this paper a comprehensive study of the pinning properties of 2 μm thick SmBCO tape grown by co-evaporation is presented [8]. The J_c and the flux creep rates are analyzed. Using electrical transport the pinning by CD was observed as a peak in the angular dependence of J_c. The J_c values at different temperatures with two different magnetic field configurations ($\mathbf{H}\|c$-axis and $\mathbf{H}\|45°$ (from c-axis)) were measured. The glassy exponents μ with $\mathbf{H}\ \|\ c$-axis and $\mathbf{H}\|45°$ (from c-axis) and magnetic fields of 5, 10 and 20 kOe were determined. Although it was observed that CD assists pinning when $\mathbf{H}\|c$, tilted angles (with lower J_c values) present poorer in-field dependences and higher flux creep rates. Our study contributes to an overall understanding of the vortex dynamics for pinning produced at different angles by CD and NPs in CCs produced by co-evaporation.

2. Experimental

The SmBCO tape was grown using the co-evaporation technique previously described in [8]. The microstructure of the films was studied by transmission electron microscopy (TEM) using a FEI Tecnai F20 G2 microscope operating at 200 kV, equipped with EDAX detector for energy-dispersive x-ray spectrometry (EDS). TEM cross sectional specimens were

prepared by a microscope/focused ion beam dual beam system (FEI Helios Nanolab 650), operated at a 2 kV voltage.

The magnetization (**M**) measurements were performed with a superconducting quantum interference device (SQUID) magnetometer with the applied magnetic field (**H**) parallel to the c-axis ($\mathbf{H} \| c$) and 45° tilted to the c-axis ($\mathbf{H} \| 45°$). A T_c value of 94 K was determined from $M(T)$ at $H = 5$ Oe applied after zero field cooling. The J_c values were calculated from the magnetization data using the appropriate geometrical factor in the Bean Model. For $\mathbf{H} \,||\, c$, $J_c = \frac{20\Delta M}{tw^2(l - w/3)}$, where ΔM is the difference in magnetization between the top and bottom branches of the hysteresis loop, and l and w are the length and the width of the single crystal ($l > w$), respectively. For $\mathbf{H}$||45°, both the longitudinal (M_l, parallel to **H**) and transverse (M_t, perpendicular to **H**) components of **M** were measured. Then we calculated the irreversible magnetization as $\Delta M = (\Delta M_l^2 + \Delta M_t^2)^{1/2}$. Using the anisotropic version of the critical state Bean model $J_c = \frac{20\Delta M}{tw^2\left(l - \frac{w\cos(45°)}{3}\right)}$ was obtained [31]. The flux creep measurements for both magnetic configurations were recorded for 1 h. The initial critical state for each creep measurement was generated using $\Delta H \sim 4H^p$, where H^p is the field for full-flux penetration [26]. For transport studies, a standard four-terminal transport technique was used to measure the angular dependence of J_c in liquid nitrogen ($T = 75.5$ K at Los Alamos National Laboratory) with a 1 μV cm^{-1} criterion (maximum Lorentz force configuration). It is important to mention that, a same specimen was used for structural, magnetic and transport studies. Initially, a piece of approximately 10 cm was used for transport studies, and then it was divided into several pieces for structural and magnetic characterization.

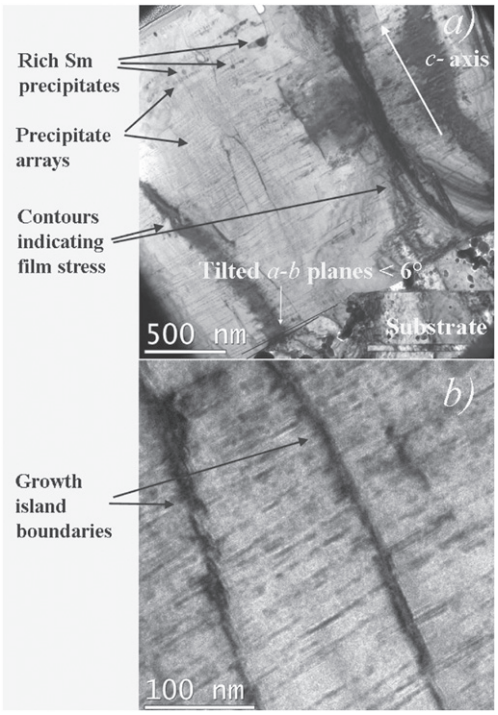

Figure 1. (a) A TEM image shows typical pinning centers in the SmBCO tape. Also the tilted a–b planes respect the substrate surface are indicated. (b) A higher magnification image shows the precipitates, boundaries between islands and stacking faults present in the sample.

3. Results and discussion

Figures 1(a) and (b) show bright field cross-section TEM images of the microstructure for the SmBCO tape. The different types of pinning centers are indicated by arrows. The microstructure presents a high density of staking faults (planar defects), dislocations, boundaries between islands (mainly aligned along the c-axis) and small precipitates or NPs. The NPs present a typical diameter 5–10 nm. According to local EDS analyses, the NPs are rich in Sm (possibly Sm_2O_3). Higher magnification images reveal a high density of ab-plane stacking faults. The cross-sectional view indicates that arrays of precipitates form 'planes' tilted at angles smaller than 6° to the IBAD template. The size of the precipitates is ~2–4 times larger than the vortex core diameters 2ξ, which produced strong pinning at temperatures above liquid nitrogen [14]. On the other hand, correlated pinning is expected along the boundaries between adjacent islands, dislocations and twin boundaries [2, 32]. The combination of different types of defects is known to be beneficial for vortex pinning [12, 14, 18, 19]. When the applied magnetic field (which determines the orientation of the vortices) is aligned with these defects, the influence of CD is expected to be strong and it decreases as the misalignment between defects and vortices increases. The presence of random point defects and NPs enhance the pinning and make it relatively uniform for all the fields [14, 20].

Figure 2(a) presents $J_c(\theta)$ for $H = 4.3$ and 8.8 kOe at 75.5 K. Both fields fall within the α power-law regime discussed below. The angular dependence shows two peaks: one centered at $\mathbf{H} \| ab$ and the other, at $\mathbf{H} \| c$. The former can be attributed to the electronic anisotropy and planar defects (staking faults). The latter indicates uniaxial pinning by c-axis CD [12]. CD is expected from twin boundaries, dislocations and boundaries between islands showed in figures 1(a) and (b). The peak $\mathbf{H} \| c$ is usually wider for mixed pinning landscapes [12]. It is also noticeable that the $J_c(\theta)$ peaks do not always fall at the expected $\mathbf{H} \| a$–b position (parallel to substrate surface) nor at the perpendicular position [33]. The misalignment between the externally applied field H and the internal field B leads to a drift of the peak position and a variation of T and H. On the other hand, the asymmetric J_c around the peak corresponding to $\mathbf{H}//a$–b position can also be associated with misalignments between the film and the substrate produced by the IBAD process included in the tape fabrication [8]. Figure 2(b) shows $J_c(H)$ for $\theta = 0$, 45° and 92°. For all the angles, a clear power-law decay ($J_c \propto H^{-\alpha}$) is observed. The α values θ from −5° to 95° are included in the inset. The values range from $\alpha \approx 0.45$ to $\alpha \approx 0.64$. The minimum α corresponds to $\mathbf{H} \| c$ and $\mathbf{H} \| a$–b. Interestingly, the maximum α value (poor in-field dependence) occurs at

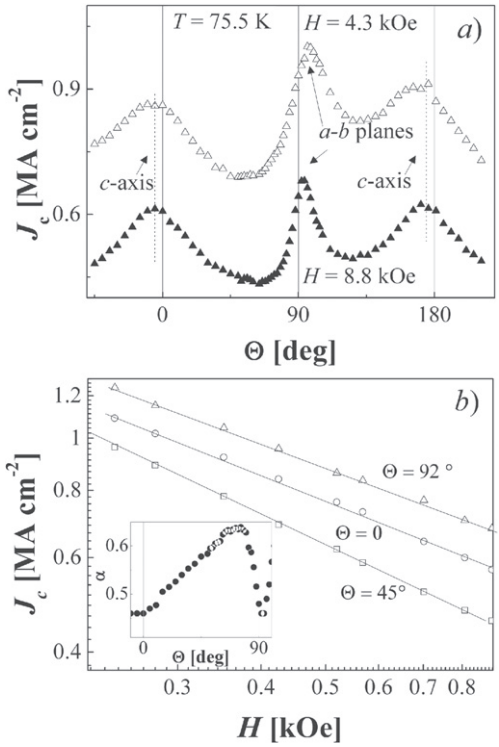

Figure 2. (a) Angular dependence of the critical current density (J_c versus θ) for $H = 4.3$ kOe and $H = 8.8$ kOe for a 2 μm thick SmBCO coated conductor. (b) J_c field dependence for H applied at $\theta = 0°$, 45° and 92°. Inset shows the angular dependence of the α exponent by considering a power-law dependence ($J_c \propto H^{-\alpha}$).

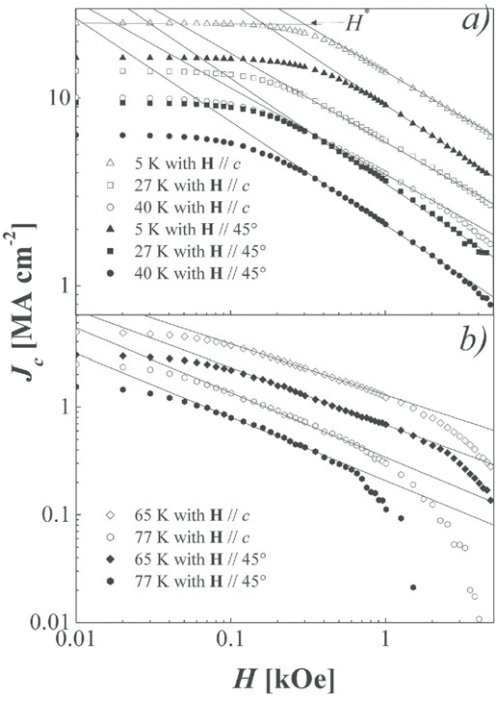

Figure 3. Magnetic field dependence of the critical current density J_c for the 2 μm thick SmBCO coated conductor at different temperatures with $\mathbf{H} \| c$ and $\mathbf{H} \| 45°$. For a clearer presentation the data was divided in two panels: (a) 5, 27 and 40 K. (b) 65 and 77 K.

$\theta \approx 70°$, which corresponds to the minimum $J_c(\theta)$ at the different fields (see figure 2(a)).

For a better understanding of the vortex dynamics in the film, J_c (H, t) dependences at different temperatures with $\mathbf{H} \| c$ and $\mathbf{H} \| 45°$ were measured for fields smaller than 50 kOe. For $\mathbf{H} \| c$, the synergetic combination CD and NPs was expected to produce the strongest pinning [12, 14]. For angles tilted from $\mathbf{H} \| c$, a reduction of the pinning by CD was expected [12]. The $J_c(H)$ dependences obtained by magnetization and electrical transport can be substantially different due to effects associated to the flux dynamics or vortex creep and the sensitivity of each method [34, 35]. For magnetization measurements, magnetic field inhomogeneities along the DC scan could affect the vortex dynamics, especially at low J_c values [34, 35]. The influence of the vortex creep should be relevant at high temperatures and high fields, which can affect the α values. Figures 3(a) and (b) show a summary of the data obtained at 5, 27, 40, 65 and 77 K. According to the magnetization curves and the Beam model, $J_c^{\|c-\text{axis}}$ is higher than $J_c^{\|45°}$ for all temperatures. This is in agreement with $J_c(\theta)$ showed in figure 2(a), which indicates that CD (associated with TBs, dislocations and boundaries between islands) acts as sources of pinning from low temperatures to 77 K. The values of $J_c^{\|c-\text{axis}}$ are 26 MA cm^{-2} and 2.5 MA cm^{-2} at 5 K and 77 K, respectively. According to the model, the $J_c^{\|45°}$ values at low fields drop around 35% in comparison with those obtained with $J_c^{\|c-\text{axis}}$. The $J_c(H)$ dependences at different temperatures present different regimes. At low fields (regime (I)), J_c is nearly constant up to a characteristic crossover field H^* (usually called B^* [36]), followed by a power-law regime ($J_c \propto H^{-\alpha}$) at intermediate fields (regime II), observed as a linear dependence on the log–log plot. Regime I (with $J_c(H) \approx$ constant) is usually associated with the single vortex pinning regime (negligible vortex–vortex interaction). However, it is also affected by self-field effects [37] and it will not be discussed. As regime II (manifested as a power-law regime) determines the in-field performance of superconductors it is highly considered of technological relevance [18]. The α exponent depends on the type of defects and it usually raises when the temperature is increased (increment in the vortex fluctuations) [12, 14, 15, 28, 36]. Finally, at temperatures above 40 K a crossover ($H^{\alpha-\text{end}}$) from the power-law regime to a regime III at which $J_c(H)$ drops faster is observed (more evident at 65 and 77 K). The observation of the regime III at lower temperatures than 40 K is limited by the maximum field of the magnetometer (50 kOe). The regime III is usually associated with fast creep relaxation and it is affected by the film thickness as well as by the type and density of pinning centers [28, 29]. It is important to mention that, due to an increment in the flux creep rates, the absolute J_c values estimated at regime III should be affected by the characteristic time involved in the DC SQUID measurements. Above $H^{\alpha\text{-end}}$ (T), the pinning strength is strongly reduced and the flux creep rates are faster [28, 29].

Figure 4 shows a summary of the $\alpha(T)$ at both magnetic field configurations for data obtained from magnetization and

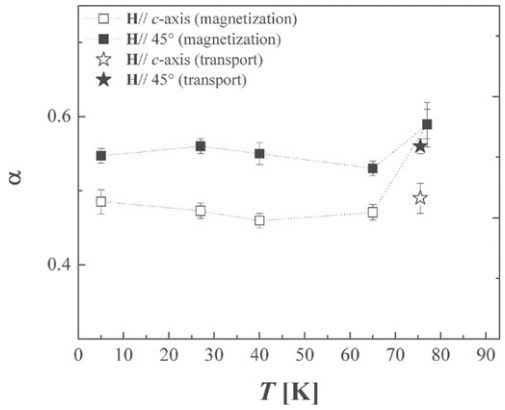

Figure 4. Temperature dependence of the α exponent for the 2 μm thick SmBCO coated conductor with $\mathbf{H}\|c$ and $\mathbf{H}\|45°$. The values are obtained from the fits presented in figure 2(b) and figures 3(a) and (b).

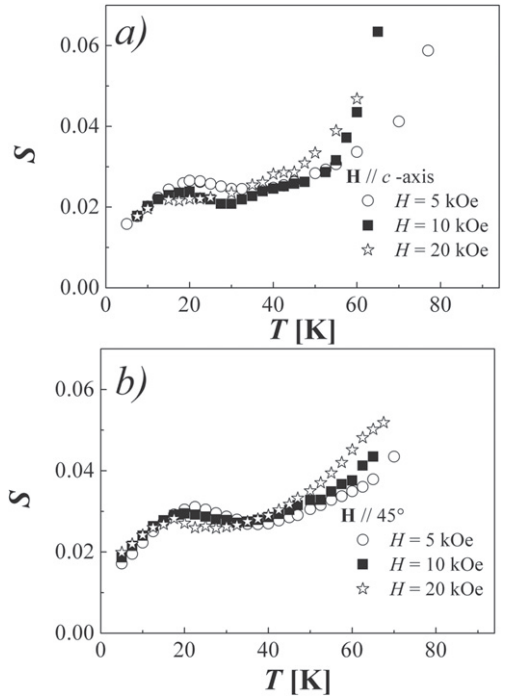

Figure 5. Temperature dependence of the creep flux rate (S) at $H = 5$, 10 and 20 kOe for the 2 μm thick SmBCO coated conductor. (a) $\mathbf{H}\|c$. (b) $\mathbf{H}\|45°$.

from electrical transport (only at $T = 75.5$ K) . The α values at low temperatures are ≈0.47 and ≈0.55 for $\mathbf{H}\|c$ and $\mathbf{H}\|45°$, respectively. The difference between α at both configurations can be ascribed to the type of pinning centers. An α value = 0.55 has been theoretically predicted for pinning for NPs [36]. For samples with CD, α can decrease to values as low as 0.2 [12, 28]. The pinning with $\mathbf{H}\|c$ is given by CD (island and twin boundaries) and NPs, which reduce α in comparison with the $\mathbf{H}\|45°$ configuration. For this configuration, the pinning is mainly settled by uncorrelated nanoprecipitates.

The vortex dynamics for the 2 μm thick SmBCO tape was analyzed by flux creep rate measurements at different temperatures and magnetic fields with $\mathbf{H}\|c$ axis and $\mathbf{H}\|45°$ (see figures 5(a) and (b)). The initial increment of S (T) at low temperatures can be ascribed to an Anderson–Kim-like mechanism with $S \approx T/U$. When the temperature is increased to ≈25 K, the measurements with $\mathbf{H}\|c$ present a peak. The peak is suppressed when H is increased from 5 to 10 kOe, and it disappears for 20 kOe. The presence of CD could associate this peak with double-excitations and also explain its appearance for $\mathbf{H}\|45°$ [12]. The plateau ($S \approx$ constant) at intermediate temperatures can be associated with glassy relaxation. The S values at the plateau ($S \approx 1/\mu \ln(t/t_0)$) are smaller for $\mathbf{H}\|c$ (≈0.024) than for $\mathbf{H}\|45°$ (≈0.028). The difference can be related to the effectiveness of the pinning centers and with the characteristic μ exponent for each magnetic configuration. Finally, when the temperature is increased, the creep rates are faster due to an increment in the thermal fluctuations and a decrease in the effective pinning energy [28, 29]. As mentioned above, the differences in the vortex dynamics at intermediate temperatures can be inferred from the μ glassy exponent, which can be inferred from Maley's analysis for each field and configuration [38]. The effective activation energy $U_{\mathrm{eff}}(J)$ can be experimentally obtained considering the approximation in which the current density decays as $\frac{\mathrm{d}J}{\mathrm{d}t} = -\left(\frac{J_c}{\tau}\right)\mathrm{e}^{-\frac{U_{\mathrm{eff}}(J)}{T}}$. The final equation for the pinning energy is

$$U_{\mathrm{eff}} = -T\left[\ln\left|\frac{\mathrm{d}J}{\mathrm{d}t}\right| - C\right], \tag{4}$$

where $C = \ln(J_c/\tau)$ is a nominally constant factor. For an overall analysis it is necessary to consider the function G (T), which results in $U_{\mathrm{eff}}(J,\ T=0) \approx U_{\mathrm{eff}}(J, T)/G(T)$ [39]. Above the peak corresponding to double kink excitations (≈25 K) and in the glassy regime, $J \ll J_c$. Figures 6(a) and (b) show the Maley analyses for both magnetic configurations, where $C = 15$ and a G (T) were used (see figures 6(a) and (b) insets). Thus, the μ exponent can be estimated as $\Delta\ln U(J)/\Delta\ln J$ [40] and μ values 1.70 ± 0.03 and 1.32 ± 0.03 were found for the $\mathbf{H}\|c$ axis and $\mathbf{H}\|45°$, respectively. Using equation [1], $\ln(t/t0) \approx 27$ was obtained for both orientations [19]. Unsubstantial μ (H) dependences were found, which is in agreement with $\mu \approx$ constant for fields corresponding to the power-law regime [19, 28].

The results indicate that the SmBCO tape presents strong pinning in the overall range of temperature, which is manifested in smooth $\alpha(T)$ dependences for T over 65 K. The poorest magnetic field configurations for the pinning (small J_c) were found to correspond to the poorest in-field dependences (higher α values). The characterizing glassy μ exponents were determined for two different angles and magnetic fields lower than 20 kOe, obtaining μ values 1.70 ± 0.03 and 1.32 ± 0.03 for the $\mathbf{H}\|c$ axis and $\mathbf{H}\|45°$, respectively. Within the studied range of fields (⩽2 T), the glassy exponents show negligible magnetic field dependence and plateau $S(H) \approx$ constant. Although CD assists pinning and improves the $J_c(H)$ dependences for the $\mathbf{H}\|c$ configuration, both absolute J_c values and α exponents are affected by the angle and the pinning drops at intermediate angles between $\mathbf{H}\|c$

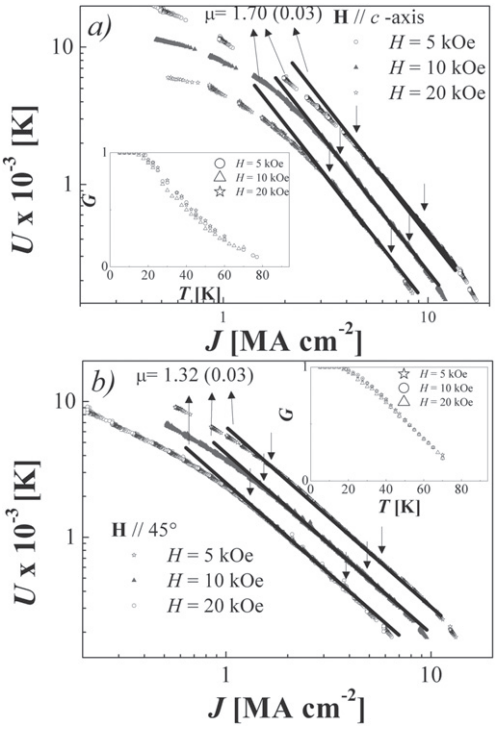

Figure 6. Maley analysis at $H = 5$, 10 and 20 kOe for the 2 μm thick SmBCO coated conductor. (a) $\mathbf{H} \| c$. (b) $\mathbf{H} \| 45°$. The insets show the $G(T)$ dependence used for the Maley analysis. Dow arrows indicate the regions where linear dependences were identified.

and $\mathbf{H} \| a$–b. This large anisotropy on the pinning properties is expected to reduce the performance of CCs for specific applications in which isotropic pinning is desired. A recent study in co-evaporated $GdBa_2Cu_3O_{7-d}$ CCs [13] reveals that the pinning landscape can be strongly modified during the synthesis. The precipitation of Gd_2O_3 nanoparticles can be modified by changing the chemical composition of the tapes. For comparison, on a 1.3 μm thick $GdBa_2Cu_3O_{7-d}$ wire, J_c ($H = 0$, 77 K) ~3.6 MA cm^{-2} was obtained [19]. The smaller value of J_c ($H = 0$, 77 K) ~ 2.5 MA cm^{-2} of 2 μm thick SmBCO could be related to thickness effects [2] and changes in the microstructure. In addition, the pinning and $J_c(H)$ dependences in CCs can be improved by the inclusion of random uncorrelated disorder by proton and oxygen irradiation [18, 19, 41]. However, despite the great advances in the fabrication of CCs, the J_c values are limited by flux creep. Therefore, the searching for methods to reduce creep and understanding of the connection between flux creep and J_c must be considered an important aspect of pinning engineering. To extend the present study and the analysis of the flux creep mechanisms (low depinning excitations), in CCs with other pinning landscapes, constitute an important factor in the rationalization of the phenomenology.

4. Summary

In summary, we have analyzed the vortex dynamics for a 2 μm thick SmBCO CC with mixed pinning landscape. The main pinning sources are CD (twin boundaries and island boundaries) and random NPs. The contribution of CD to the pinning was directly verified from $J_c(\theta)$ at 75.5 K by electrical transport. In addition, we have studied $J_c(H)$ at different temperatures for the $\mathbf{H} \| c$ and $\mathbf{H} \| 45°$ configurations by performing magnetic measurements. We have found that CD contributes to the pinning throughout the range of temperature (from 5 to 77 K). The presence of CD improves the $J_c(H)$ when $\mathbf{H}$ is aligned with the defects. The α value is affected by the angle and the pinning drops at intermediate angles between $\mathbf{H} \| c$ and $\mathbf{H} \| a$–b. Finally, a high contribution to the pinning is expected from planar defects and stacking faults. The α values drop at $\mathbf{H} \| 45°$, which can be related to a large vortex–vortex interaction. We have found that the glassy exponent for $\mathbf{H} \| c$ is $\mu = 1.70 \pm 0.03$ whereas for $\mathbf{H} \| 45°$, it is $\mu = 1.32 \pm 0.03$. According to $J_c(\theta)$ at liquid nitrogen, poorer magnetic field dependences and faster creep relaxation are expected for $\theta \approx 70°$. To further improve the J_c properties for some specific technological applications (i. e. magnets), a smaller J_c anisotropy is desired, which can be induced by a large contribution of randomly distributed NPs to the $J_c(\theta)$ dependences. In addition, the extension of the present study to samples grown by other methods is necessary to understand the role of the microstructure in the resulting vortex dynamics of CCs.

Acknowledgments

We thank A Geraci for technical assistance with TEM. NH is a member of the Instituto de Nanociencia y Nanotecnología (Argentina).

References

[1] Larbalestier D, Gurevich A, Feldmann D M and Polyanskii A 2001 *Nature* **414** 368
[2] Foltyn S R, Civale L, MacManus-Driscoll J L, Jia Q X, Maiorov B, Wang H and Maley M 2007 *Nat. Mater.* **6** 631
[3] Durrell J H *et al* 2014 *Supercond. Sci. Technol.* **27** 082001
[4] Trociewitz U P, Dalban-Canassy M, Hannion M, Hilton D K, Jaroszynski J, Noyes P, Viouchkov Y, Weijers H W and Larbalestier D C 2011 *Appl. Phys. Lett.* **99** 202506
[5] Rupich M W, Verebelyi D T, Zhang W, Kodenkandath T and Li X 2004 *MRS Bull.* **29** 572
[6] Obradors X, Puig T, Ricart S, Coll M, Gazquez J, Palau A and Granados X 2012 *Supercond. Sci. Technol.* **25** 123001
[7] Selvamanickam V *et al* 2009 *IEEE Trans. Appl. Supercond.* **19** 3225
[8] Oh S S *et al* 2008 *Supercond. Sci. Technol.* **21** 034003
[9] Kang S *et al* 2006 *Science* **311** 1911
[10] Matsumoto K and Mele P 2010 *Supercond. Sci. Technol.* **23** 014001
[11] Holesinger T G *et al* 2008 *Adv. Mater.* **20** 391
[12] Maiorov B, Baily S A, Zhou H, Ugurlu O, Kennison J A, Dowden P C, Holesinger T G, Foltyn S R and Civale L 2009 *Nat. Mater.* **8** 398
[13] MacManus-Driscoll J L *et al* 2014 *APL Mater.* **2** 086103

[14] Miura M, Maiorov B, Baily S A, Haberkorn N, Willis J O, Marken K, Izumi T, Shiohara Y and Civale L 2011 *Phys. Rev.* B **83** 184519
[15] Macmanus-Driscoll J L, Foltyn S R, Jia Q X, Wang H, Serquis A, Civale L, Maiorov B, Hawley M E, Maley M P and Peterson D E 2004 *Nat. Mater.* **3** 439
[16] Pan V *et al* 2006 *Phys. Rev.* B **73** 054508
[17] Albrecht J, Djupmyr M and Brück S 2007 *J. Phys.: Condens. Matter* **19** 216211
[18] Jia Y *et al* 2013 *Appl. Phys. Lett.* **103** 122601
[19] Haberkorn N, Kim J, Suárez S, Lee J-H and Moon S H 2015 *Supercond. Sci. Technol.* **28** 125007
[20] Gutierrez J *et al* 2006 *Nat. Mater.* **6** 367
[21] Feldmann D M, Ugurlu O, Maiorov B, Stan L, Holesinger T G, Civale L, Foltyn S R and Jia Q X 2007 *Appl. Phys. Lett.* **91** 162501
[22] Koshelev A E and Kolton A B 2011 *Phys. Rev.* B **84** 104528
[23] Civale L *et al* 2004 *Appl. Phys. Lett.* **84** 2121
[24] Chen Z, Kametani F, Gurevich A and Larbalestier D 2009 *Phys.* C **469** 2021
[25] Blatter G, Feigel'man M V, Geshkenbein V B, Larkin A I and Vinokur V M 1994 *Rev. Mod. Phys.* **66** 1125
[26] Yeshurun Y, Malozemoff A P and Shaulov A 1996 *Rev. Mod. Phys.* **68** 911
[27] Selvamanickam V *et al* 2013 *Supercond. Sci. Technol.* **26** 035006
[28] Haberkorn N *et al* 2012 *Phys. Rev.* B **85** 174504
[29] Rouco V *et al* 2014 *Supercond. Sci. Technol.* **27** 115008
[30] Eley S *et al* 2016 Decoupling and tuning competing effects of different types of defects on flux creep in irradiated $YBa_2Cu_3O_{7-\delta}$ coated conductors arXiv:1602.04344
[31] Haberkorn N *et al* 2012 *Phys. Rev.* B **85** 014522
[32] Dam B, Huijbregtse J M and Rector J H 2002 *Phys. Rev.* B **65** 064528
[33] Maiorov B, Gibbons B J, Kreiskott S, Matias V, Holesinger T G and Civale L 2005 *Appl. Phys. Lett.* **86** 132504
[34] Pan A V, Golovchanskiy A I and Fedoseev S A 2013 *EPL* **103** 17006
[35] Golovchanskiy I A, Pan A V, Shcherbakova O V and Fedoseev S A 2013 *J. Appl. Phys.* **114** 163910
[36] van der Beek C J, Konczykowski M, Abal'oshev A, Abal'osheva I, Gierlowski P, Lewandowski S J, Indenbom M V and Barbanera S 2002 *Phys. Rev.* B **66** 024523
[37] Haberkorn N *et al* 2011 *Phys. Rev.* B **84** 94522
[38] Maley M P, Willis J O, Lessure H and McHenry M E 1990 *Phys. Rev.* B **42** 2639
[39] Ossandon J G, Thompson J R, Christen D K, Sales B C, Sun Y and Lay K W 1992 *Phys. Rev.* B **46** 3050
[40] Thompson J R, Krusin-Elbaum L, Civale L, Blatter G and Field C 1997 *Phys. Rev. Lett.* **78** 3181
[41] Leroux M *et al* 2015 *Appl. Phys. Lett.* **107** 192601